Identification of Manganese Superoxide Dismutase from *Sphingobacterium sp.* T2 as a Novel Bacterial Enzyme for Lignin Oxidation

Goran M. M. Rashid,[1] Charles R. Taylor,[1] Yangqingxue Liu,[1] Xiaoyang Zhang,[1] Dean Rea,[2] Vilmos Fülöp,[2] and Timothy D. H. Bugg[1]*

Department of Chemistry[1] and School of Life Sciences[2],
University of Warwick, Coventry CV4 7AL, United Kingdom.

*Corresponding author: Prof. T.D.H. Bugg, Department of Chemistry, University of Warwick, Coventry CV4 7AL, U.K. Tel 44-2476-573018. Email T.D.Bugg@warwick.ac.uk

Keywords: lignin valorisation; lignin oxidation; manganese superoxide dismutase; *Sphingobacterium*

Abstract: The valorisation of aromatic heteropolymer lignin is an important unsolved problem in the development of a biomass-based biorefinery, for which novel high-activity biocatalysts are needed. Sequencing of the genomic DNA of lignin-degrading bacterial strain *Sphingobacterium sp.* T2 revealed no matches to known lignin-degrading genes. Proteomic matches for two manganese superoxide dismutase proteins were found in partially purified extracellular fractions. Recombinant MnSOD1 and MnSOD2 were both found to show high activity for oxidation of Organosolv and Kraft lignin, and lignin model compounds, generating multiple oxidation products. Structure determination revealed that the products result from aryl-C_α and C_α-C_β bond oxidative cleavage and *O*-demethylation. The crystal structure of MnSOD1 was determined to 1.35 Å resolution, revealing a typical MnSOD homodimer harbouring a 5-coordinate trigonal bipyramidal Mn(II) centre ligated by three His, one Asp and a water/hydroxide in each active site. We propose that the lignin oxidation reactivity of these enzymes is due to the production of hydroxyl radical, a highly reactive oxidant. This is the first demonstration that MnSOD is a microbial lignin-oxidising enzyme.

Introduction

The aromatic heteropolymer lignin is an important component of lignocellulose matrix of plant cell walls, comprising 15-30% dry weight of lignocellulose.[1] Lignin is liberated during physicochemical pretreatment of biomass for cellulosic bioethanol production, and is also produced industrially from pulp/paper manufacture via the Kraft process, but is currently a low value by-product that is burnt for energy or used in the production of concrete, asphalt, and polymeric materials.[1,2] The aromatic content of lignin is a potentially valuable source of renewable aromatic chemicals, and the valorisation of lignin via either chemical or biocatalytic routes is of considerable current interest, but has proved very challenging.[2]

Microbial degradation of lignin has been mainly studied in basidiomycete fungi: white-rot fungi such as *Phanerochaete chrysosporium* produce extracellular lignin peroxidase and manganese peroxidase enzymes that can oxidise lignin, and some fungi produce extracellular laccases that can also attack lignin.[1] Despite reports of bacterial oxidation of lignin,[3,4] until recently the enzymology of bacterial lignin breakdown (summarised in Figure 1) was poorly understood. In 2011 we reported a dye-decolorising peroxidase DypB from *Rhodococcus jostii* RHA1 that played a significant role in the lignin-degrading ability of this strain, and the recombinant protein was shown to oxidise both Mn(II) and lignin model compounds, catalysing oxidative C_α-C_β bond cleavage of a β-aryl ether lignin dimer.[5] A further Dyp2 peroxidase has been identified in *Amycolatopsis* sp. 75iv2 that shows higher activity for Mn(II) oxidation.[6] Bacterial laccase enzymes have also been identified in *Streptomyces coelicolor* A3(2), *S. viridosporus* T7A, and *Amycolatopsis* sp. 75iv2, which catalyse C_α oxidation of a lignin model compound, and whose genetic knockout significantly reduces the ability of the host to metabolise lignin.[7] Given the complexity of the lignin polymer, it seems likely that there is a group of lignin-oxidising enzymes, and that further lignin-oxidising enzymes are still to be discovered.

Figure 1. Bacterial enzymes for lignin oxidation

Using a colorimetric assay method,[8] we have previously reported a screening method for isolation of lignin-oxidising bacterial strains from environmental soil samples.[9] Using this method we reported the isolation of 12 novel bacterial lignin-oxidising strains, including a thermotolerant *Sphingobacterium* sp. T2 isolate which grows on minimal media containing wheat straw lignocellulose as sole carbon source,[9] or minimal media containing Kraft lignin (see Supporting Information S1), and which showed >10-fold higher activity for lignin oxidation than other isolates in our assay.[9] Another *Sphingobacterium* isolate with high activity for lignosulfonate degradation has also subsequently been reported.[10] In this paper we report the identification from proteomic

analysis and genome sequencing of two extracellular manganese superoxide dismutase enzymes in *Sphingobacterium* sp. T2 that show novel reactivity for lignin oxidation.

Results

Proteomic analysis of Sphingobacterium sp. T2

Extracellular fractions of *Sphingobacterium* sp. T2 grown on Luria-Bertani broth were partially purified via Q sepharose anion exchange and phenyl sepharose hydrophobic interaction chromatography. Several active fractions were observed (see Supporting Information S2), which showed activity using both the nitrated lignin colorimetric assay[8] and ABTS oxidation. Proteomic analysis via tryptic digestion and MALDI-MS peptide identification, followed by matching to libraries of genomic data, gave a number of matching sequences from *Sphingobacterium spiritovorum* strains ATCC 33300 and ATCC 33861, *Leadbetterella byssophila* DSM 17132, *Pedobacter* sp. BAL39 and *Chryseobacterium gleum*. The list of proteins (see Supporting Information Figure S3) includes proteins OmpA and TonB, both known to be major cell surface proteins in *Bacteroides fragilis,*[11,12] and several enzyme activities. Of particular interest are two sequences for manganese superoxide dismutase. Although there are no reports of superoxide dismutase involvement in lignin breakdown, this enzyme catalyses the interconversion of dioxygen with reactive oxygen species superoxide and peroxide,[13] consistent with an observation that *Sphingobacterium* T2 showed higher lignin oxidation activity in the presence of dioxygen, rather than hydrogen peroxide.[9]

The genomic DNA sequence of *Sphingobacterium* sp. T2 (deposited as DDBJ/EMBL/GenBank accession JXAC00000000) contains two genes encoding manganese superoxide dismutases, named as *sod1* and *sod2*, matching the proteomic amino acid sequences obtained above. Both encoded proteins showed sequence similarity to the SodA family of superoxide dismutases, with Sod1 and Sod2 showing 49% and 47% sequence identity to *E. coli* SodA respectively, and 73% sequence identity to each other. The Sod1 amino acid sequence contains a 25 amino acid N-terminal protein targeting sequence MMKMNIFKTALVATALFATQTTFA identified by software SignalP 4.0. In the *Sphingobacterium* sp. T2 genome sequence, *sod1* is located adjacent to an ECF sigma factor and anti-sigma factor regulatory genes, while *sod2* is located within a cluster of 14 genes containing two *araC* regulatory genes and three ABC transporter component genes (see Supporting Information Figure S24). The genome contains no dyp-type peroxidase genes and no putative laccase genes, and no recognisable aromatic degradation gene clusters, quite different to the genome sequence of *Rhodococcus jostii* RHA1, which contains large numbers of gene clusters for aromatic degradation.[14] The only annotated peroxidase genes are: a catalase/peroxidase (KatG) of the same

class as an enzyme reported to show activity for oxidation of a lignin model compound[15]; glutathione peroxidase; cytochrome c peroxidase; a thiol peroxidase and an alkylhydroperoxidase. We therefore decided to express recombinant enzyme for the two MnSOD enzymes, and the catalase/peroxidase KatG enzyme.

Expression and assay of KatG. MnSOD1, and MnSOD2

The genes encoding *Sphingobacterium sp*. T2 KatG, MnSOD1 and MnSOD2 were amplified by PCR and expressed as His_6 fusion proteins in *E. coli*. In the case of MnSOD1, removal of the N-terminal signal sequence was found to aid protein expression in *E. coli*. Each recombinant protein expressed as soluble protein and was purified by metal affinity chromatography, giving yields of 3.8, 19.5 and 23 mg protein/L culture respectively (see Supporting Information Figures S4 & S7).

Recombinant *Sphingobacterium* KatG was purified as an 86 kDa protein, was found to be active for oxidation of guaiacol (2-methoxyphenol, v_{max} 0.005 µmol min^{-1} mg $protein^{-1}$, K_m 2.1 mM) and ABTS (v_{max} 0.006 µmol min^{-1} mg $protein^{-1}$, K_m 5.3 µM) in the presence of 4 mM hydrogen peroxide (see Supporting Information Figure S5), and showed weak activity for oxidation of bromophenol blue, bromothymol blue, and reactive black 5 dyes. However, recombinant KatG showed no detectable reaction with wheat straw lignocellulose or alkali Kraft lignin, by HPLC analysis, hence this enzyme does not appear to be responsible for the lignin oxidation activity of *Sphingobacterium* sp. T2.

Recombinant *Sphingobacterium* MnSOD1 and MnSOD2 were purified as 22.6 and 20.3 kDa proteins respectively. The recombinant enzymes were found to be active for superoxide dismutation, as measured by inhibition of pyrogallol auto-oxidation (1,2,3-trihydroxybenzene, specific activities: SOD1 400 units/mg; SOD2 124 units/mg)[16], and inhibition of cytochrome c oxidation (specific activities: SOD1 3090 units/mg; SOD2 860 units/mg).[17] Both purified recombinant proteins showed some UV-vis absorbance peaks in the range 360-600 nm: recombinant SOD1 is a pale pink colour, showing a weak absorbance peak at 465 nm (ε = 470 $M^{-1}cm^{-1}$), comparable to reported λ_{max} values of 480 nm for the human[18] and *Anabaena*[19] MnSOD enzymes; recombinant SOD2 is colourless, but shows absorbance peaks at 411 nm and 503 nm (see Supporting Information Figures S8, S9).

Analysis of metal content using ICP-MS revealed that recombinant SOD1 contained 91% total metal content as Mn, with 7.4% Fe. In contrast, recombinant SOD2 was found to contain 54.7% Zn, 22.6% Mn, 18.4% Fe and 4.9% Cu. In order to investigate the metal dependence of SOD2 for activity, 20µM SOD2 apoenzyme was incubated with $FeSO_4$, $CuSO_4$ or $MnSO_4$ in molar

ratios of 1:4, 1:2, 1:1 and 2:1 metal ion: enzyme ratio. Activity using the pyrogallol assay was only observed in the presence of Mn^{2+}, with optimum activity requiring 1-2 molar equivalents of Mn^{2+} (see Supporting Information S10).

Upon incubation of 720 µg SOD1 or SOD2 with a suspension of Organosolv lignin in 50 mM potassium phosphate buffer 7.8, to which was added 1.25 mM KO_2, a visible change in colour from yellow to orange was observed over 60 min, and a change in the solubility of the lignin was observed, becoming noticeably more water soluble (see Figure 2A). Analysis of reaction components by reverse phase HPLC revealed the presence of a number of new peaks, together with an envelope of products in the range 6-20 min with increasing intensity vs. time, as shown in Figure 2B. Reaction was also observed with alkali Kraft lignin, generating multiple reaction products (Supporting Information Figure S11). There was a slow background reaction in the presence of KO_2 alone, but the background reaction generated only a small envelope of products in the range 12-20 min retention time (see Figure 2B), with much smaller individual product peaks. SOD1 and SOD2 also showed activity for lignin oxidation in the presence of 1 mM hydrogen peroxide under aerobic conditions, which would be formed by spontaneous dismutation of superoxide in aqueous solution. Treatment of organosolv lignin under these conditions generated the same reaction products, but the peak intensities were only 10% of those obtained in the presence of KO_2 over a 60 min incubation. The rate of consumption of organosolv lignin was estimated as 0.86 mg/min/mg SOD1; assuming an average molecular weight of 200 amu for an aryl-C_3 lignin unit, this corresponds to a rate of 99 µmol lignin units/min/µmol enzyme, or an apparent rate constant of 1.64 s^{-1}.

Figure 2. Reaction of organosolv lignin with MnSOD.

Analysis of the reaction products from processing of Organosolv lignin by GC-MS gave 10 new product peaks, which were identified by comparison with authentic standards, as shown in Figure 3 (see Supporting Information Figures S12-S21). Products vanillic acid (**1**), dihydroxybenzoic acid (**2**), 5-hydroxyvanillic acid (**3**), 4-hydroxybenzoic acid (**4**) and vanillin (**5**) result from cleavage of the C_α-C_β bond in lignin aryl-C_3 units, while 2-methoxyhydroquinone (**7**) guaiacol (**8**), and catechol (**9**) result from cleavage of the aryl-C_α bond in lignin aryl-C_3 units. 4-(2-hydroxyethyl)guaiacol (**6**) contains an aryl-C_2 skeleton but is deoxygenated at C_β. Oxalic acid (**10**) has been observed previously as a metabolite of microbial lignin oxidation.[8,20] For the background reaction in the presence of KO_2 only, the only product peaks that could be detected by GC-MS were small amounts of vanillic acid (**1**) and oxalic acid (**10**), as shown in Figure 3.

In order to study which of the observed products may be derived from the predominant β-aryl ether (β-O-4) linkage present in polymeric lignin, incubations of SOD1 and SOD2 with a β-

aryl ether model compound guaiacylglycerol-β-guaiacyl ether were carried out. Products 2-methoxyhydroquinone (**7**) and guaiacol (**8**) were observed, consistent with aryl-C_α bond cleavage. Incubation of SOD1 or SOD2 with guaiacol (**8**) gave catechol (**9**) as product, indicating that the oxidative demethylation of guaiacol is catalysed by SOD1 and SOD2.

In order to examine whether the lignin oxidation activity was unique to the *Sphingobacterium* MnSOD enzymes, manganese superoxide dismutase genes from *Escherichia coli* and *Thermus thermophilus* were cloned and overexpressed in *E. coli* as His_6 fusion proteins, and the purified recombinant enzymes were assayed (see Supporting Information S22). When incubated with organosolv lignin and KO_2, only very small amounts of product metabolites were observed by HPLC analysis, corresponding to 5-6% of the products formed by SpMnSOD1, similar to the background KO_2 reaction.

The generation of multiple reaction products implies the generation of a reactive oxidant by the *Sphingobacterium* MnSOD enzymes. In order to investigate turnover-dependent enzyme inactivation, SOD activity was measured under the lignin oxidation conditions, using the pyrogallol assay. It was found that 75% activity was lost after 30 min under these conditions, but thereafter 10-20% residual activity was retained over 3-4 hr (see Supporting Information S28). Analysis of recombinant SpMnSOD1 by electrospray mass spectrometry verified the expected mass at 26,394 Da, which was still the major species present after 1 hr under the assay conditions (see Supporting Information S24), indicating that there is no rapid chemical modification of the enzyme.

Figure 3. Reaction products obtained from treatment of organosolv lignin by SOD1 and SOD2

Crystal structure of MnSOD1

Diffracting crystals of *Sphingobacterium sp* T2 MnSOD (SpMnSOD1) were obtained, and X-ray diffraction data collected to 1.35 Å. The structure of SpMnSOD1 was determined using molecular replacement using the MnSOD structure from *Bacillus subtilis* (pdb: 2RCV).[23] The crystal structure of SpMnSOD1 revealed a typical MnSOD homodimer comprising two characteristic Fe/MnSOD subunits (Figure 4). The SpMnSOD1 monomers superpose with an rmsd of 0.108 Å (165 CA atoms), and are therefore essentially structurally identical. The SpMnSOD1 monomer and dimer share high structural homology with other MnSOD enzymes for which crystal structures have been determined. Structural superposition of SpMnSOD1 with homologs from *E. coli* (pdb code 1D5N),[21] *T. thermophilus* (pdb code 3MDS),[22] *B. subtilis* (pdb code 2RCV),[23] *D. radiodurans* (pdb code 1Y67),[24] and the filamentous cyanobacterium *Anabena* PCC 7120 (pdb code 1GV3)[25] gave an rmsd of ~0.4-0.7 Å for the monomer, and ~0.5-0.9 Å for the dimer (Figure 4).

Figure 4. Structure of SpMnSOD1, superimposed onto other MnSOD structures

Each SpMnSOD1 subunit contains a 5-coordinate trigonal bipyramidal Mn ion ligated by His26 and water/hydroxide as apical ligands, and His76, Asp163 and His167 as equatorial ligands (Figure 5A). The Mn ligands and inner sphere residues are surrounded by outer sphere residues including the highly conserved so-called "gateway" residues.[26] In SpMnSOD1 these include His30, Tyr34 and Gln144, along with Glu166 and Tyr170 from the other monomer of the homodimer (Figure 5A). Of these, Gln144 that is bound to the axial water/hydroxyl ligand is known to be important for catalytic activity in the *E. coli* enzyme,[27] and Glu166 is known to be required for both dimerization and activity in the *T. thermophilus* enzyme.[28]

Figure 5. Active site of SpMnSOD1

Dimerization of MnSOD subunits is mediated by interactions between His30 of chain A and Tyr170 of chain B, and between His167 of chain A and Glu166 of chain B (see Figure 5A).[21] The His30A-Tyr174B interaction may allow each monomer to influence or coordinate catalysis in the other active site,[26] while the hydrogen bond between His167A and Glu166B results in a pair of bridges between the two Mn centres.[21] All of the Mn ligands and gateway residues are conserved in the primary sequence, and can be superimposed with only very small perturbations in structure (see Figure 5B). However, there are some amino acid replacements near the active site, shown in Figure 6. In the vicinity of Mn ligand His-26, residues His-27 and His-31 of EcMnSOD are replaced in SpMnSOD1 by Tyr and Ala respectively; near Mn ligand His-76, Ala-74 is replaced by Tyr in both SpMnSOD1 and SpMnSOD2; and Ser-77 is replaced by either Glu (in SpMnSOD1) or Lys (in SpMnSOD2).

Figure 6. Partial amino acid sequence alignment of MnSOD enzymes, showing replacements near His-26 and His-76

Conclusions

Proteomic analysis of extracellular fractions from *Sphingobacterium* sp. T2 has identified two extracellular manganese superoxide dismutase enzymes, which in recombinant form are both highly active for oxidation of Organosolv lignin, generating multiple reaction products. This is a surprising observation, since superoxide dismutase was believed to function only in cellular protection against oxidative stress,[13] so lignin oxidation is a new function for superoxide dismutase. The presence of two highly active lignin-oxidising enzymes in this strain may therefore explain the

high activity of this isolate, and also explains the observed lignin degradation activity of this isolate in the absence of hydrogen peroxide.[9]

The presence of an extracellular superoxide dismutase enzyme is unusual, since bacterial superoxide dismutases are usually intracellular,[13] however an extracellular MnSOD enzyme has been reported in *Streptococcus pyogenes*,[29] which shares 42% and 48% sequence identity with SpMnSOD1 and SpMnSOD2 respectively. Database searches using the BLAST algorithm (see Supporting Information Figures S25, S26) reveal that homologues for SpMnSOD1 and SpMnSOD2 are found the Sphingobacteriales and Flavobacteriales, and also in strains of *Acinetobacter* (γ-proteobacteria). Interestingly, an extracellular manganese superoxide dismutase has been reported in a gene cluster for metabolism of poly(*cis*-1,4-isoprene) in *Gordonia polyisoprenivorans* VH2, and is required for efficient growth on poly(*cis*-1,4-isoprene) as carbon source.[30] Schulte et al proposed that the SodA enzyme is probably involved in protection against reactive oxygen species during rubber breakdown,[30] but this enzyme also shares 32% and 37% sequence identity with SpMnSOD1 and SpMnSOD2 respectively, so it might also possess oxidative C-C bond cleavage activity. Given the close similarity in structure between the *Sphingobacterium* MnSOD enzymes and *E. coli* and *T. thermophilus* MnSOD enzymes, it is interesting that the latter enzymes are much less active for lignin oxidation, implying that there is some special reactivity possessed by the *Sphingobacterium* MnSOD enzymes.

Following lignin oxidation by superoxide dismutase enzymes, the subsequent metabolism of the lignin oxidation products is unclear, since the genome of *Sphingobacterium* sp. T2 does not appear to contain any conventional aromatic degradation gene clusters. We have previously found that this strain is able to utilise vanillic acid as sole carbon source for growth,[9] which suggests that it is able to metabolise such intermediates. The reaction products that we have observed from oxidation of Organosolv lignin are highly oxidised, so we suspect there may be a pathway similar to the phloroglucinol pathway observed in *Pelobacter acidigallici* (Bacteroidaceae),[31] *Eubacterium oxidoreducens*,[32] and *Coprococcus* sp.,[33] in which a 1,3,5-trihydroxybenzene tautomerises to a non-aromatic cyclohexane-1,3,5-trione, which is then a substrate for hydrolytic cleavage, rather than oxidative ring cleavage.

Treatment of Organosolv lignin with Sod1 or Sod2 generates multiple reaction products, of which we have characterised 12 structures shown in Figure 3. The formation of the reaction products shown in Figure 2 from lignin indicates that aryl-C_α oxidative bond cleavage has taken place (products **7**-**10**), as well as C_α-C_β oxidative cleavage (products **1**-**5**), decarboxylation (e.g. conversion of **1** to **9**) and *O*-demethylation (products **2**, **10**). The generation of such a range of reaction products and reaction types from Organosolv or Kraft lignin implies the generation of a highly reactive oxidant. The reaction cycle of manganese superoxide dismutase, shown in Figure 5,

involves two half-reactions, namely oxidation of superoxide to dioxygen by Mn(III), and reduction of superoxide to hydrogen peroxide by Mn(II).[13,18,19] Two possible hypotheses for interaction with lignin are illustrated in Figure 7. The first possibility (Figure 7A) is that the Mn(III) form of the metal cofactor might oxidise lignin, analogous to the generation of Mn(III) by fungal manganese peroxidase, which then acts as a diffusible oxidant to attack lignin.[34] However, the manganese cofactor in superoxide dismutases is generally tightly bound, and we have seen no evidence that it is released by the *Sphingobacterium* SOD enzymes.

Figure 7. Hypotheses for generation of lignin oxidant by MnSOD

The second hypothesis (Figure 7B) is that the SpMnSOD enzymes are able to further reduce peroxide to hydroxyl radical, which is the reactive oxidant to attach lignin. It is reported that bovine erythrocyte Cu/Zn superoxide dismutase can generate hydroxyl radical, but that *E. coli* MnSOD, which in our hands shows very little lignin oxidation activity, does not generate hydroxyl radical.[35] The observation of oxidation products containing additional phenolic hydroxyl groups (e.g. products **3**, **6**, **7**) is consistent with the known ability of hydroxyl radical to carry out phenolic hydroxylation,[36] hence this appears to be a possible mechanism for lignin oxidation via these enzymes. We note that Nature uses hydroxyl radical to attack lignin in a different context: brown rot fungi utilise Fenton chemistry to generate hydroxyl radical to attack lignin.[37,38] There are also literature reports of the production of hydroxyl radical in white rot fungus *Phanerochaete chrysosporium*,[39-41] though subsequent data implied that this is not a major contributing mechanism in white-rot fungal lignin degradation.[42]

We therefore propose a possible mechanism shown in Figure 8 for the generation of the observed products from Organosolv lignin. Hydroxyl radical is reported to cause demethoxylation of methoxylated aromatic compounds, via addition of hydroxyl radical to the aromatic ring.[37] If hydroxyl radical attacked at aryl C-1 of an aryl-C_3 unit, then C-C fragmentation as shown in Figure 8 would generate compound **7**, observed in incubations of SpMnSOD enzymes with both Organosolv lignin and a β-aryl ether model compound. Hydroxyl radical is also known to cause oxidative fragmentation of ketones such as α-oxo-γ-methylthiobutyric acid,[41,43] therefore we propose that oxidative cleavage of a benzylic ketone intermediate could lead to vanillic acid **1** via cleavage **A**, and guaiacol **8** via cleavage **B**. Demethoxylation of guaiacol **8**, a known reaction for hydroxyl radical,[37] would generate catechol **9**. Further hydroxylation of vanillic acid **1**, a known reaction for hydroxyl radical,[36] would then generate 5-hydroxyvanillic acid **3**.

Figure 8. Mechanism for generation of reaction products from Organosolv lignin

The crystal structure of *Sphingobacterium* sp. T2 MnSOD1 determined here shows high structural similarity with MnSOD structures from *E. coli* and *T. thermophilus*, that we have shown experimentally to have low activity for lignin oxidation. Hence we suggest that amino acid replacements near to the active site may affect the environment of the active site and perhaps alter the redox potential of these enzymes, leading to a change in reactivity of these enzymes. There are several amino acid replacements close to Mn ligands His-26 and His-76 (see Figure 6) that would potentially change the charge balance near the active site, whose precise function will be studied in future work. Another unsolved question is how the enzyme protects itself from chemical modification by the hydroxyl radical oxidant that is generated. We have shown that turnover-dependent inactivation of the enzyme does occur to some extent, but not completely (see Supporting Information Figure S23). Furthermore, there is no chemical modification of the polypeptide observed by mass spectrometry (see Supporting Information Figure S24), nor in the crystal structure of SpMnSOD1.

The identification of the *Sphingobacterium* sp. T2 manganese superoxide dismutases as lignin-oxidising enzymes expands the range of bacterial enzymes capable of lignin oxidation.[5-7] These enzymes could be valuable biocatalysts for the valorisation of lignin produced as a by-product of biofuel production and pulp/paper manufacture, including Kraft lignin for which the SpMnSOD enzymes show activity.[4] The identification of reaction products from oxidation of polymeric lignin helps to define further the metabolic pathways for microbial lignin breakdown.[20]

Methods

Proteomic analysis. Cultures of *Sphingobacterium* sp T2 were grown in Luria-Bertani broth (1.5 litre) at 45 °C for 24 hr. After centrifugation (6,000 g, 20 min), protein was precipitated by addition of 70% ammonium sulfate, followed by centrifugation (15,000 g, 20 min). Pellets were re-suspended in 20 mM potassium phosphate buffer (pH 7.4), applied to a Q sepharose anion exchange column, and eluted in a gradient of 0-2 M NaCl in 20 mM potassium phosphate buffer (pH 7.4), at a flow rate of 1.6 ml min^{-1}. The flow-through fraction from the Q sepharose column was most active, and was further purified by Phenyl Sepharose column chromatography, eluting with 20 mM sodium phosphate (pH 7.4) containing a gradient of 2 M to 0 M $(NH_4)_2SO_4$ at a flow rate of 1.6 ml min^{-1}. Fractions were assayed for activity using the nitrated lignin assay in the presence and absence of H_2O_2.[8] Active fractions were analysed by SDS-PAGE (see Supporting Information S2), and Coomassie-stained gel bands were processed and proteomic analysis carried out by the WPH Proteomics Facility (School of Life Sciences, University of Warwick). After tryptic digestion, the extracted peptides from each sample were analyzed by nano LC-ESI-MS/MS using Nano

Acquity/Ultima Global Instrumentation (Waters), using a 30 min LC gradient. The data were processed to generate peak list files using Protein Lynx Global Server v 2.5.1. The observed molecular ion data for tryptic digests were compared with protein databases, and a number of matches were found (see Supporting Information Figure S3).

Expression of recombinant KatG and MnSOD1&2.

Cloning primers were designed for the *Sphingobacterium* sp. T2 *katG*, *sod1* and *sod2* genes, and *E. coli* and *T. thermophilus* MnSOD containing a 5'-CACC overhang (see Supporting Information S4, S7, S23 for primer sequences). The *katG, sod1* and *sod2* genes were amplified from *Sphingobacterium* sp. T2 genomic DNA by polymerase chain reaction, using Platinum Pfx-DNA polymerase from Invitrogen, following manufacturer's instructions. The amplified genes were cloned using the Champion™ pET Directional TOPO® Expression Kit (Invitrogen) into expression vector pET200 (*katG*) or pET151 (*sod1, sod2, EcSOD, TtSOD*), and transformed into *Escherichia coli* DH5α (*katG*) or TOP10 competent cells (Invitrogen). The recombinant plasmids were then transformed into BL21 *E. coli* BL21(DE3)pLysS (Invitrogen), for protein expression.

Cultures of each recombinant strain were grown at 37 ºC in 500 ml Luria-Bertani media containing 40 µg/ml kanamycin (for KatG) or 100 mg/ml ampicillin, induced with 0.5 mM IPTG (isopropyl-β-D-thiogalactopyranoside) at OD_{600} = 0.6, then incubated overnight at 15ºC with shaking at 180 rpm. In the case of SOD1 and SOD2, 1mM $MnSO_4$ was also added at induction. The cell pellet was harvested by centrifugation (6000 g, 15 min). The cells were resuspended in 20 mM Tris pH 8.0 containing 10 mM imidazole, 0.5 M NaCl, 1 mM PMSF, passed through a cell disruptor, centrifuged (10,000 g, 35 min), and the supernatant was filtered with a Whatman® 0.2 µM syringe filter. The soluble protein fraction was loaded on to a 5 ml pre-equilibrated Ni-NTA column (Qiagen) with 20 mM Tris pH 8.0 buffer containing 20 mM imidazole, 0.5 M NaCl, and eluted with 20 mM Tris pH 7.8 containing 300 mM imidazole, 0.5 M NaCl. The purified enzyme was concentrated with an Amicon centrifugal unit (10kDa cut off), and de-salted with a PD-10 column, eluting with 50mM sodium phosphate buffer pH 7.8.

Enzyme assays. KatG assay was carried out in 1 mL of 50 mM sodium acetate (pH 5.0) containing 0.5 mM ABTS, 4.0 mM H_2O_2, to which was added recombinant KatG. Reactions were monitored at 414 nm (ε_{414} = 36,600 $M^{-1}cm^{-1}$). Guaiacol oxidation was carried out in 1 mL of 50 mM sodium acetate (pH 5.0) containing 100 µM guaiacol, 4.0 mM H_2O_2, to which was added recombinant KatG, monitoring at 465 nm (ε_{465} = 26,600 $M^{-1}cm^{-1}$). SOD activity was assayed via inhibition of pyrogallol auto-oxidation[16] in 50mM Tris buffer pH 8.2 containing 0.1 mM EDTA, or via ferricytochrome assay[17] in 50 mM phosphate buffer (pH 7.8) containing 0.1 mM EDTA, 50 µM xanthine, 20 µM cytochrome c, and 0.01 units xanthine oxidase.

Incubation with lignin or lignin model compounds. Solutions of 5mg of wheat straw Organosolv lignin or alkali Kraft lignin or powdered miscanthus lignocellulose (5 mg/ml in DMSO) or lignin model compound (10 mg/ml in methanol) were prepared. Reactions were carried out in a 3 ml volume using 50mM NH_4HCO_3 buffer pH 7.8 containing 0.1 mM EDTA, containing either 200uL lignin model compound or 500uL lignin sample, and 0.8 mg SOD enzyme. 1mL of a saturated solution of KO_2 in dry DMSO (5 mM) was added to start the reaction. A control incubation was also prepared in which the SOD enzyme is replaced by buffer. Reactions were incubated at 30 ^oC for 5 hours, at which point 200uL 1M HCl was added to stop the reaction and precipitate the enzyme. No activity was observed using boiled enzyme, nor with the same molar concentration of $MnSO_4$.

Analysis of reaction products. After stopping the enzyme reaction as described above, samples were centrifuged (13000 rpm, microcentrifuge) for 10min prior to analysis by HPLC. HPLC method A: analysis was conducted using a Phenomenex Luna 5 μm C18 reverse phase column (4.6 mm) on a Hewlett-Packard Series 1100 analyzer, at a flow rate of 0.5 mL/min, with monitoring at 310 nm. The gradient was as follows: 20 to 30% MeOH/H_2O over 5 min, 30 to 50% MeOH/H_2O from 5 to 12 min, and 50 to 80% MeOH/H_2O from 12 to 25 min. Method B: column and flow rate as above, monitoring at 270 and 310 nm. Buffer A: H_2O with 0.1% v/v formic acid; buffer B, MeOH. Gradient: start with 5% buffer B, 5-30%B over 0-20 min; 30%B for 10 min; 30-100%B for 15 min; 100%B for 8 min; 100-5%B over 8 min. Reaction products were extracted into ethyl acetate, and the organic layer was evaporated. The products dissolved in chloroform, dried (Na_2SO_4), and filtered. The samples were analysed by LC-MS or by GC-MS, either directly or after derivatisation with N,O-bis(trimethylsilyl)acetamide (see Supporting Information S12).

Crystallization and structure determination of SpMnSOD1. Methods for protein crystallisation, X-ray data collection, structure determination and refinement are described in Supporting Information S29, with crystallographic data and refinement statistics.

Acknowledgements. The authors wish to thank the Kurdistan Regional Government (KRG) Ministry of Higher Education and Scientific Research (PhD studentship to GMMR), the Tuck Foundation (PhD studentship to CRT), and BBSRC research grant BB/M003523/1 (to TDHB and VF) for financial support. We wish to thank L. Eltis and N. Seghezzi (University of British Columbia) for communication of the genomic DNA sequence for *Sphingobacterium* sp. T2 prior to deposition. We thank S. Slade for proteomic analysis at the WPH Proteomics Facility (School of

Life Sciences, University of Warwick). Crystallographic data were collected at beam line IO3 at Diamond Light Source, UK and we acknowledge the support of the beam line scientists.

References

1. Wong, D.W.S. (2009) Structure and action mechanism of lignolytic enzymes. *Appl. Biochem. Biotechnol*. *157*, 174-209.
2. Zakzeski, J., Bruijnincx, P.C., Jongerius, A.L., and Weckhuysen, B.M. (2010) The catalytic valorization of lignin for the production of renewable chemicals. *Chem. Rev. 110*, 3552–3599.
3. Ramachandra, M., Crawford, D., and Hertel, G. (1988) Characterization of an extracellular lignin peroxidase of the lignocellulolytic actinomycete *Streptomyces viridosporus*, *Appl. Environ. Microbiol. 54*, 3057-3063.
4. Bugg, T.D.H., Ahmad, M., Hardiman, E.M., and Singh, R. (2011) The emerging role for bacteria in lignin degradation and bio-product formation. *Curr. Opin. Biotech*. *22*, 394-400.
5. Ahmad, M., Roberts, J.N., Hardiman, E.M., Singh, R., Eltis, L.D., and Bugg, T.D.H. (2011) Identification of DypB from *Rhodococcus jostii* RHA1 as a lignin peroxidase. *Biochemistry 50*, 5096-5107.
6. Brown, M.E., Barros, T., and Chang, M.C.Y. (2012) Identification and characterization of a multifunctional dye peroxidase from a lignin-reactive bacterium. *ACS Chem. Biol*. *7*, 2074-2081.
7. Majumdar, S., Lukk, T., Bauer, S., Nair, S.K., Cronan, J.E., and Gerlt, J.A. (2014). Roles of small laccases from *Streptomyces* in lignin degradation. *Biochemistry 53*, 4047-4058.
8. Ahmad, M., Taylor, C.R., Pink, D., Burton, K., Eastwood, D., Bending, G.D., and Bugg, T.D.H. (2010) Development of novel assays for lignin degradation: comparative analysis of bacterial and fungal lignin degraders, *Mol. Biosystems 6*, 815-821.
9. Taylor, C.R., Hardiman, E.M., Ahmad, M., Sainsbury, P.D., Norris, P.R., and Bugg, T.D.H. (2012) Isolation of bacterial strains able to metabolise lignin from screening of environmental samples. *J. Appl. Microbiol*. *113*, 521-530.
10. Wang, D., Lin, Y., Du, W., Liang, J., and Ning, Y. (2013) Optimization and characterization of lignosulfonate biodegradation process by a bacterial strain, *Sphingobacterium* sp. HY-H. *Int. Biodeter. Biodeg. 85*, 365-371.
11. Wexler, H.M., Tenorio, E., and Pumbwe, L. (2009). Characteristics of *Bacteroides fragilis* lacking the major outer membrane protein OmpA. *Microbiology 155*, 2694-2706.

12. Pauer, H., Ferreira, E.O., Santos-Filho, J.D., Portela, M.B., Zingali, R.B., Soares, R.M.A., and Domingues, R.M.C. (2009). A TonB-dependent outer membrane protein as a *Bacteroides fragilis* fibronectin-binding molecule. *FEMS Immunol. Med. Microbiol. 55*, 388-395.
13. Fridovich, I. (1975). Superoxide dismutases. *Annu. Rev. Biochem. 44*, 147-159.
14. McLeod, M.P., Warren, R.L., Hsiao, W.W.L., Araki, N., Myhre, M., Femandes, C., Miyazawa, D., Wong, W., Lillquist, A.L., Wang, D., Dosanjh, M., Hara, H., Petrescu, A., Morin, R.D., Yang, G., Stott, J.M., Schein, J.E., Shin, H., Smailus, D., Siddiqui, A.S., Marra, M.A., Jones, S.J.M., Holt, R., Brinkman, F.S.L., Miyauchi, K., Fukuda, M., Davies, J.E., Mohn, W.W., Eltis, L.D. (2006). The complete genome of *Rhodococcus sp* RHA1 provides insights into a catabolic powerhouse. *Proc. Natl. Acad. Sci. USA 103*, 15582-15587.
15. Brown, M.E., Walker, M.C., Nakashige, T.G., Iavarone, A.T., and Chang, M.C.Y. (2011). Discovery and characterization of heme enzymes from unsequenced bacteria: application to microbial lignin degradation. *J. Am. Chem. Soc. 133*, 18006-18009.
16. He, Y-Z., Fan, K-Q., Jia, C-J., Wang, Z-J., Pan, W-B., Li, H., Yang, K-Q., and Dong, Z-Y. (2007). Characterization of a hyperthermostable Fe-superoxide dismutase from hot spring. *Appl Microbiol Biotechnol. 75*, 367-376.
17. McCord, J.M. and Fridovich, I. (1969). Superoxide dismutase: an enzymic function for erythrocuprein (hemocuprein). *J. Biol. Chem. 244*, 6049-6055.
18. Hsu, J-L., Hsieh, Y., Tu, C., O'Connor, D., Nick, H.S., and Silverman, D.N. (1996). Catalytic properties of human manganese superoxide dismutase. *J. Biol. Chem. 271*, 17687-17691.
19. Regelsberger, G., Atzenhofer, W., Rüker, F., Peschek, G.A., Jakopitsch, C., Paumann, M., Furtmüller, P.G., and Obinger, C. (2002). Biochemical characterization of membrane-bound manganese-containing superoxide dismutase from the cyanobacterium Anabaena PCC7120. *J. Biol. Chem. 277*, 43615-43622.
20. Bugg, T.D.H., Ahmad, M., Hardiman, E.M., and Rahmanpour, R. (2011). Pathways for degradation of lignin in bacteria and fungi. *Nat. Prod. Reports 28*, 1883-1896.
21. Edwards, R.A., Baker, H.M., Whittaker, M.M., Whittaker, J.W., Jameson, G.B., and Baker, E.N. (1998). Crystal structure of *Escherichia coli* manganese superoxide dismutase at 2.1 Å resolution. *J. Biol. Inorg. Chem. 3*, 161-171.
22. Ludwig, M.L., Metzger, A.L., Pattridge, K.A., and Stallings, W.C. (1991). Manganese superoxide dismutase from *Thermus thermophilus*: a structural model refined at 1.8 Å resolution. *J. Mol. Biol. 219*, 335-358.
23. Liu, P., Ewis, H.E., Huang, Y-J., Lu, C-D., Tai, P.C., and Weber, I.T. (2007). Structure of *Bacillus subtilis* superoxide dismutase. *Acta Cryst. F63*, 1003-1007.

24. Dennis, R.J., Micossi, E., McCarthy, J., Moe, E., Gordon, E.J., Kozielski-Stuhrmann, S., Leonard, G.A., and McSweeney, S. (2006). Structure of the manganese superoxide dismutase from *Deinococcus radiodurans* in two crystal forms. *Acta Cryst. F62*, 325-329.
25. Atzenhofer, W., Regelsberger, G., Jacob, U., Peschek, G.A., Furtmüller, P.G., Huber, R., and Obinger, C. (2002). The 2.0 Å resolution structure of the catalytic portion of a cyanobacterial membrane-bound manganese superoxide dismutase. *J. Mol. Biol. 321*, 479-489.
26. Edwards, R.A., Whittaker, M.M., Whittaker, J.W., Baker, E.N., and Jameson, G.B. (2001). Removing a hydrogen bond in the dimer interface of *Escherichia coli* manganese superoxide dismutase alters structure and reactivity. *Biochemistry 40*, 4622-4632.
27. Edwards, R.A., Whittaker, M.M., Whittaker, J.W., Baker, E.N., and Jameson, G.B. (2001). Outer sphere mutations perturb metal reactivity in manganese superoxide dismutase. *Biochemistry 40*, 15-27.
28. Whittaker, M.M. and Whittaker, J.W. (1998). A glutamate bridge is essential for dimer stability and metal selectivity in manganese superoxide dismutase. *J. Biol. Chem. 273*, 22188-22193.
29. Gerlach, D., Reichardt, W., and Vettermann, S. (1998). Extracellular superoxide dismutase from *Streptococcus pyogenes* type 12 strain is manganese-dependent. *FEMS Microbiol. Lett. 160*, 217-224.
30. Schulte, C., Arenskötter, M., Berekas, M.M., Arenskötter, Q., Priefert, H., and Steinbüchel, A. (2008). Possible involvement of an extracellular superoxide dismutase (SodA) as a radical scavenger in poly(cis-1,4-isoprene) degradation. *Appl. Environ. Microbiol. 74*, 7643-7653.
31. Brune, A. and Schink, B. (1992). Phloroglucinol pathway in the strictly anaerobic *Pelobacter acidigallici*: fermentation of trihydroxybenzenes to acetate via triacetic acid. *Arch. Microbiol. 157*, 417-424.
32. Krumholz, L.R., Crawford, R.L., Hemling, M.E., and Bryant, M.P. (1987). Metabolism of gallate and phloroglucinol in *Eubacterium oxidoreducens* via 3-hydroxy-5-oxohexanoate. *J. Bacteriol. 169*, 1886-1890.
33. Tsai, C-G., Gates, D.M., Ingledew, W.M., and Jones, G.A. (1976). Products of anaerobic phloroglucinol degradation by *Coprococcus* sp. Pe15. *Can. J. Microbiol. 22*, 159-164.
34. Ten Have, R. and Teunissen, P.J.M. (2001). Oxidative mechanisms involved in lignin degradation by white-rot fungi. *Chem. Rev., 101*, 3397-3413
35. Yim, M.B., Chock, P.B., and Stadtman, E.R. (1990). Copper, zinc superoxide dismutase catalyzes hydroxy radical production from hydrogen peroxide. *Proc. Natl. Acad. Sci. USA 87*, 5006-5010.
36. Halliwell, B. (1978). Superoxide-dependent formation of hydroxyl radicals in the presence of iron chelates. *FEBS Letters 92*, 321-326.

37. Hydre, S.M. and Wood, P.M. (1997). A mechanism for production of hydroxyl radicals by the brown-rot fungis *Coniophora puteana*: Fe(III) reduction by cellulose dehydrogenase and Fe(II) oxidation at a distance from the hyphae. *Microbiology 143*, 259-266.
38. Kerem, Z., Jensen, K.A., and Hammel, K.E. (1999). Biodegradative mechanism of the brown rot basidiomycete *Gloeophyllum trabeum*: evidence for an extracellular hydroquinone-driven Fenton reaction. *FEBS Lett. 446*, 49-54.
39. Forney, I.J., Reddy, C.A., Tien, M., and Aust, S.D. (1982). The involvement of hydroxyl radical derived from hydrogen peroxide in lignin degradation by the white rot fungus *Phanerochaete chrysosporium*. *J. Biol. Chem. 257*, 11455-11462.
40. Kutsuki, H. and Gold, M.H. (1982). Generation of hydroxyl radical and its involvement in lignin degradation by *Phanerochaete chrysosporium*. *Biochem. Biophys. Res. Commun*. *109*, 320-327.
41. Kelley, R.L. and Reddy, C.A. (1982). Ethylene production from α-oxo-γ-methylthiobutyric acid is a sensitive measure of lignolytic activity by *Phanerochaete chrysosporium*. *Biochem. J. 206*, 423-425.
42. Kirk, T.K., Mozuch, M.D., and Tien, M. (1985). Free hydroxyl radical is not involved in an important reaction of lignin degradation by *Phanerochaete chrysosporium* Burds. *Biochem. J. 226*, 455-460.
43. Digiuseppi, J. and Fridovich, I. (1980). Ethylene from 2-keto-4-thiomethylbutyric acid: the Haber-Weiss reaction. *Arch. Biochem. Biophys*. *205*, 323-329.
44. Read, R.J. (1986). Improved Fourier coefficients for maps using phases from partial structures with errors. *Acta Cryst. A42*, 140-149.
45. DeLano, W.L. (2002). The PyMOL User's Manual, DeLano Scientific, Palo Alto, CA.

Figure Legends.

Figure 1. Bacterial enzymes for oxidation of lignin.

Figure 2. Reaction of Organosolv lignin with SpMnSOD1, as described in Materials & Methods. **A.** Change in visual appearance upon addition of SpMnSOD1 and KO_2 to a solution of wheat straw Organosolv lignin (on left), compared with the control reaction with no enzyme (on right). **B.** Reaction products from reaction of SpMnSOD1 with Organosolv lignin, observed by HPLC analysis. New peaks *a-e* are observed, which were subsequently found to contain the following breakdown products: peak *a* contains compounds **2**, **3**, **4**, **7**, and **10**; peak *b* contains compounds **1** and **9**; peak *c* contains compound **8**; peak *d* contains compounds **5** and **6**; peak *e* contains unidentified compounds of *m/z* 335-414, corresponding to a mixture of lignin dimer products. Control reaction contains KO_2 but no enzyme.

Figure 3. Reaction products observed from processing of wheat straw Organosolv lignin by SpMnSOD1 and SpMnSOD2, and negative control containing no enzyme, identified by GC-MS.

Figure 4. Structure of the SpMnSOD1 homodimer (cartoon, gray) superimposed with structures of related MnSOD enzymes. Mn(II) ions are shown as purple spheres. Structures of MnSOD from *E. coli* (1D5N; salmon), *T. thermophilus* (3MDS; yellow), *B. subtilis* (2RCV; light green), *D. radiodurans* (1Y67; magenta), and *Anabena* (1GV3; cyan) are shown in ribbon representation. Figure drawn with Pymol.[45]

Figure 5. Structure of the SpMnSOD1 active site. **A.** Mn(II) is shown as a purple sphere, hydrogen bonds with the co-ordinating apical (His26 and water/hydroxide) and equatorial (His76, Asp163 and His167) ligands are indicated by dotted lines. Both the axial water/hydroxide and an additional potentially important solvent molecule bound to Tyr34 and His30 are shown as small red spheres. Carbon atoms of Glu166 and Tyr170 from the other monomer of the homodimer are coloured green. **B.** Superposition of SpMnSOD1 active site with close structural homologs *E. coli* (pdb code 1D5N; salmon; monomer superposition = 0.679 Å for 144 CA; dimer superposition = 0.859 for 302 CA); *T. thermophilus* (pdb code 3MDS; yellow; monomer superposition = 0.538 for 150 CA; dimer superposition = 0.905 for 315 CA); *B. subtilis* (pdb code 2RCV; light green; monomer superposition = 0.416 for 147 CA; dimer superposition = 0.601 for 295 CA); *D. radiodurans* (pdb code 1Y67; magenta; monomer superposition = 0.471 for 148 CA; dimer superposition = 0.481 for 295 CA); filamentous cyanobacterium *Anabena* PCC 7120 (pdb code 1GV3; cyan; monomer

superposition = 0.445 for 137 CA; dimer superposition = 0.841 for 314 CA). Numbering refers to SpMnSOD1. **C.** The SIGMAA weighted 2mFo-ΔFc electron density[44] using phases from the final model of the SpMnSOD1 Mn^{3+}-binding site is contoured at 1.0 Å level, where s represents the RMS electron density for the unit cell. Contours more than 1.4 Å from any of the displayed atoms have been removed for clarity. Figure drawn with PyMOL.[45]

Figure 6. Partial amino acid sequence alignment of SpMnSOD1 and SpMnSOD2 with extracellular SodA enzymes reported from *Streptococcus pyogenes* (STRPY), *Gordonia isoprenivorans* (GORPV), and MnSOD enzymes from *E. coli* and *Thermus thermophilus* (THET8), showing amino acid replacements (highlighted in green) in SpMnSOD1 and SpMnSOD2 close to Mn ligands His-26 and His-76 (in yellow) and active site residues His-30, Tyr-34 and Asn-75 (in cyan). Full amino acid sequence alignment shown in Supporting Information Figure S28.

Figure 7. Hypotheses for generation of lignin oxidant by SpMnSOD enzymes.

Figure 8. Mechanism for generation of reaction products **1**, **3**, **7**-**10** from Organosolv lignin (only partial structure shown). A hydrogen atom donor XH is required for formation of compound **8**, and a radical species is required to generate a phenoxy radical intermediate in the first step of the formation of compound **7**. Conversion of **1** to **3** also involves a phenoxy radical intermediate, which reacts with hydroxyl radical at C-5. Conversion of **8** to **9** also involves a phenoxy radical intermediate, which reacts with hydroxyl radical via *ipso*-substitution at C-2.

Figure 1

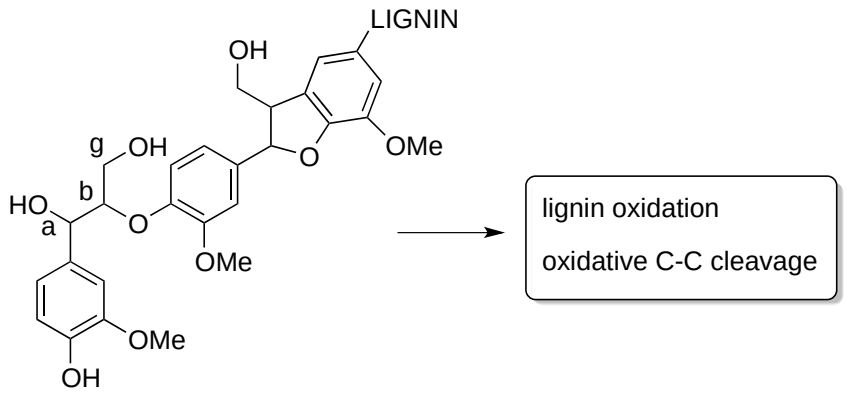

Bacterium	Enzyme	Reaction type
Rhodococcus jostii RHA1	Peroxidase DypB	Mn^{2+} oxidation, C_a-C_b cleavage
Amycolatopsis sp. 75iv2	Peroxidase Dyp2	Mn^{2+} oxidation
Streptomyces coelicolor	Laccase	C_a oxidation

Figure 2

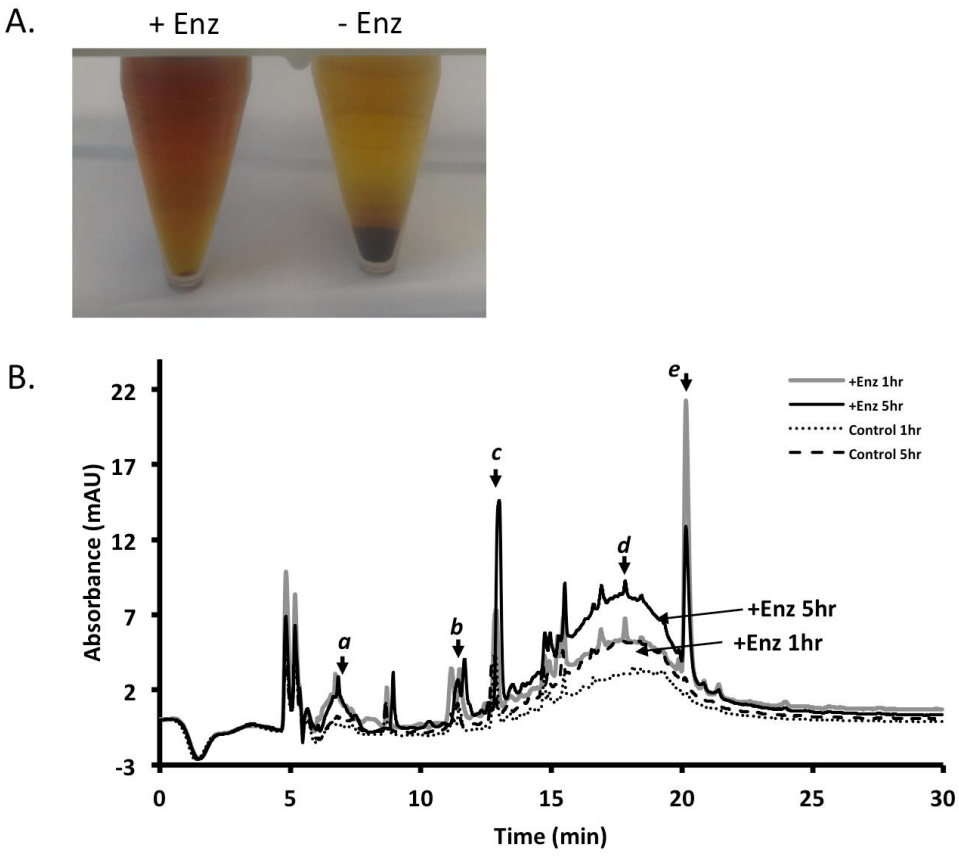
A.
+ Enz
- Enz
B.
Absorbance (mAU)
Time (min)
+Enz 1hr
+Enz 5hr
Control 1hr
Control 5hr
a
b
c
d
e
+Enz 5hr
+Enz 1hr

Figure 3

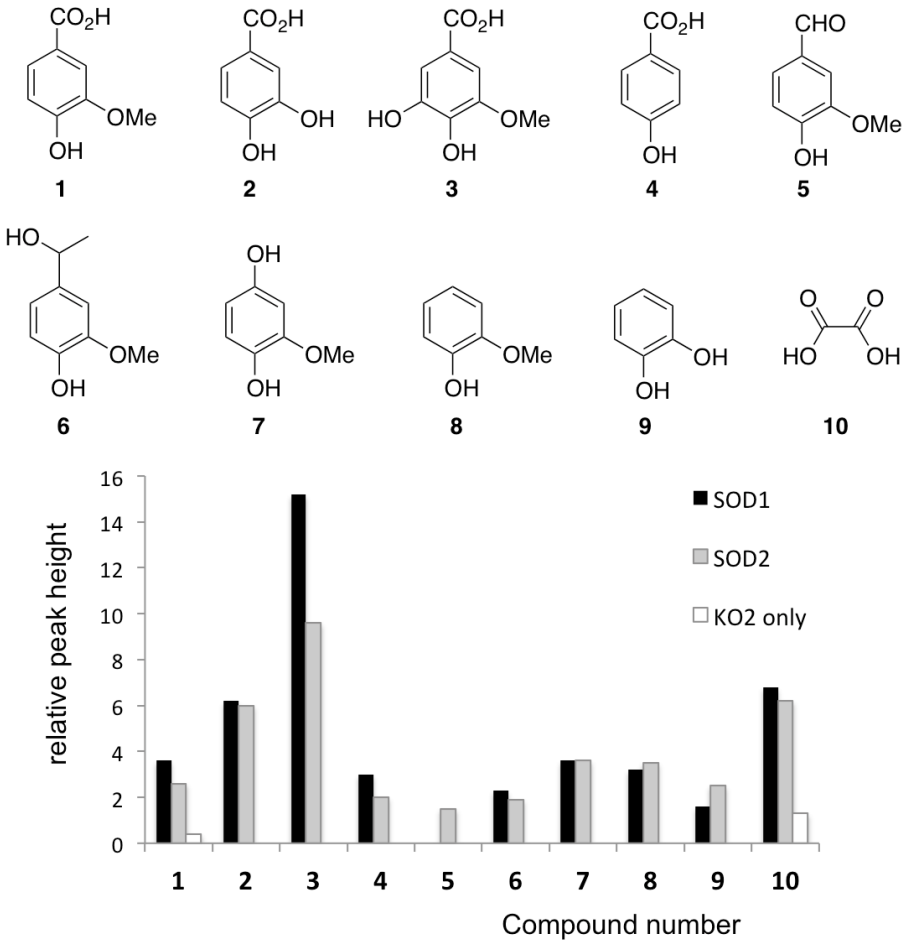
CO2H
OMe
OH
1
CO2H
OH
OH
2
CO2H
HO
OMe
OH
3
CO2H
OH
4
CHO
OMe
OH
5
HO
OMe
OH
6
OH
OMe
OH
7
OMe
OH
8
OH
OH
9
O
O
HO
OH
10
relative peak height
16
14
12
10
8
6
4
2
0
SOD1
SOD2
KO2 only
1
2
3
4
5
6
7
8
9
10
Compound number

Figure 4

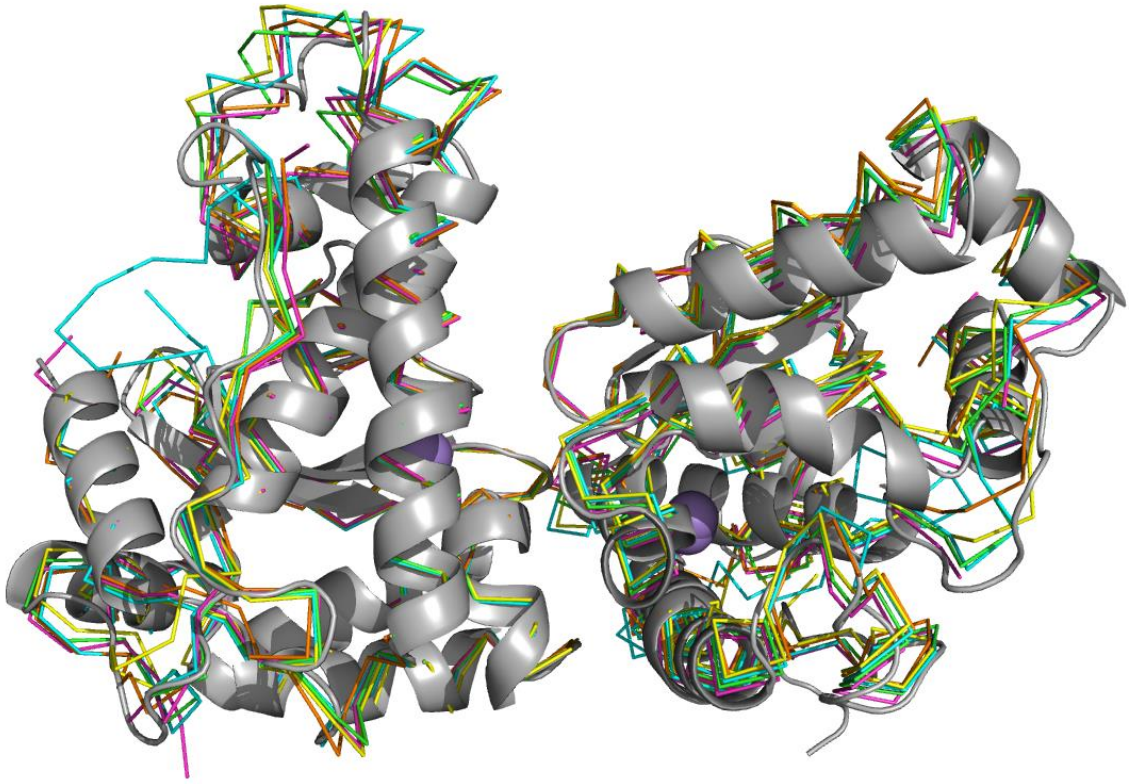

Figure 5

A.

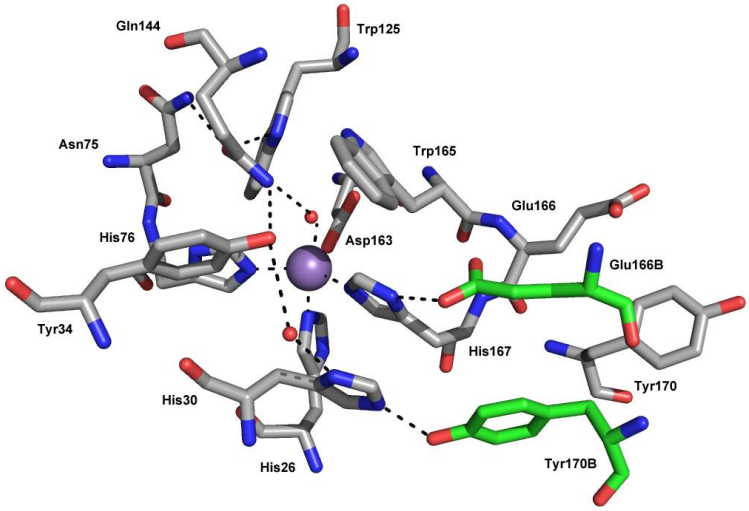
Gln144
Trp125
Asn75
Trp165
Glu166
His76
Asp163
Glu166B
Tyr34
His167
Tyr170
His30
His26
Tyr170B

B.

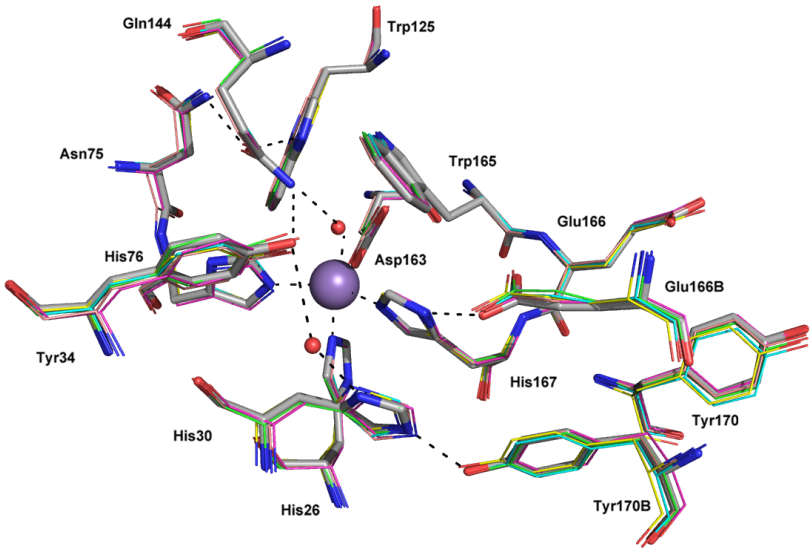
Gln144
Trp125
Asn75
Trp165
Glu166
His76
Asp163
Glu166B
Tyr34
His167
Tyr170
His30
His26
Tyr170B

C.

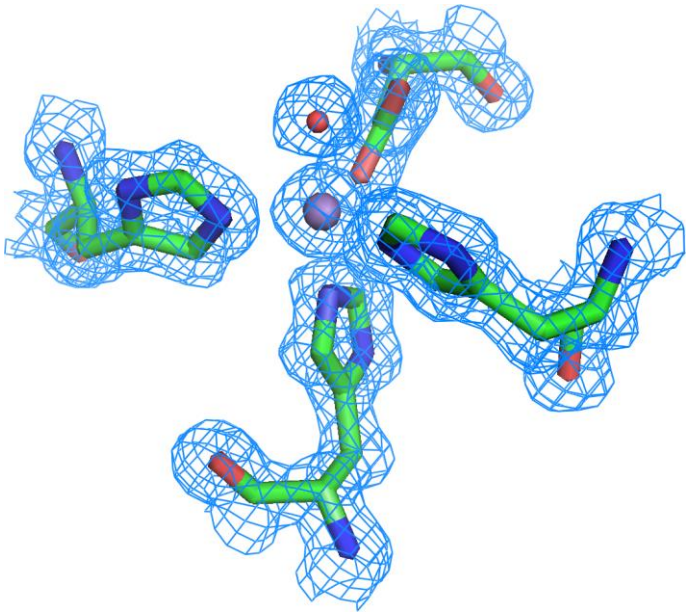

Figure 6

```
                      26                                  76
SpMnSOD1          MEIHYSKHAAGYTANLNKAI   GHYNHELFWSILTP
SpMnSOD2          MEIHHDRHHQAYVDNLNKAI   GHYNHKLFWSILSP
SODM_THET8        MEIHHQKHHGAYVTNLNAAL   GHLNHSLFWRLLTP
SODM_STRPY        MTLHHDKHHATYVANTDAAL   GHLNHALFWELLSP
SODM_ECOLI        MEIHHTKHHQTYVNNANAAL   GHANHSLFWKGLKK
H6MT45_GORPV      MELHHDKHHATYVKGANDTL   GHTNHSIFWKNLSP
                      : :*   *. . : ::   ** ** :**  *.
```

Figure 7

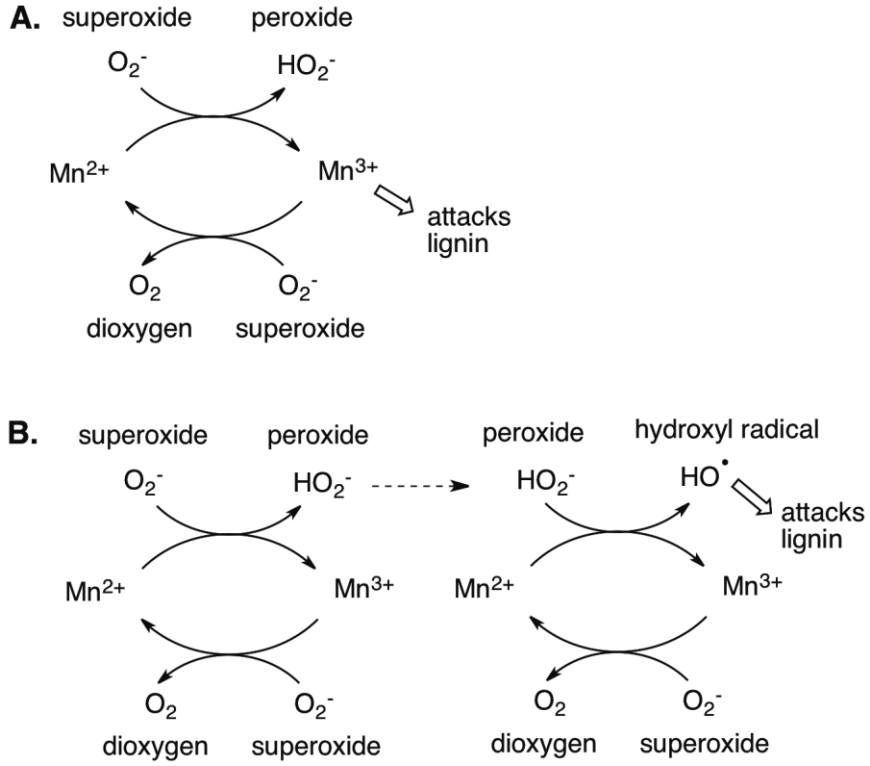

Figure 8

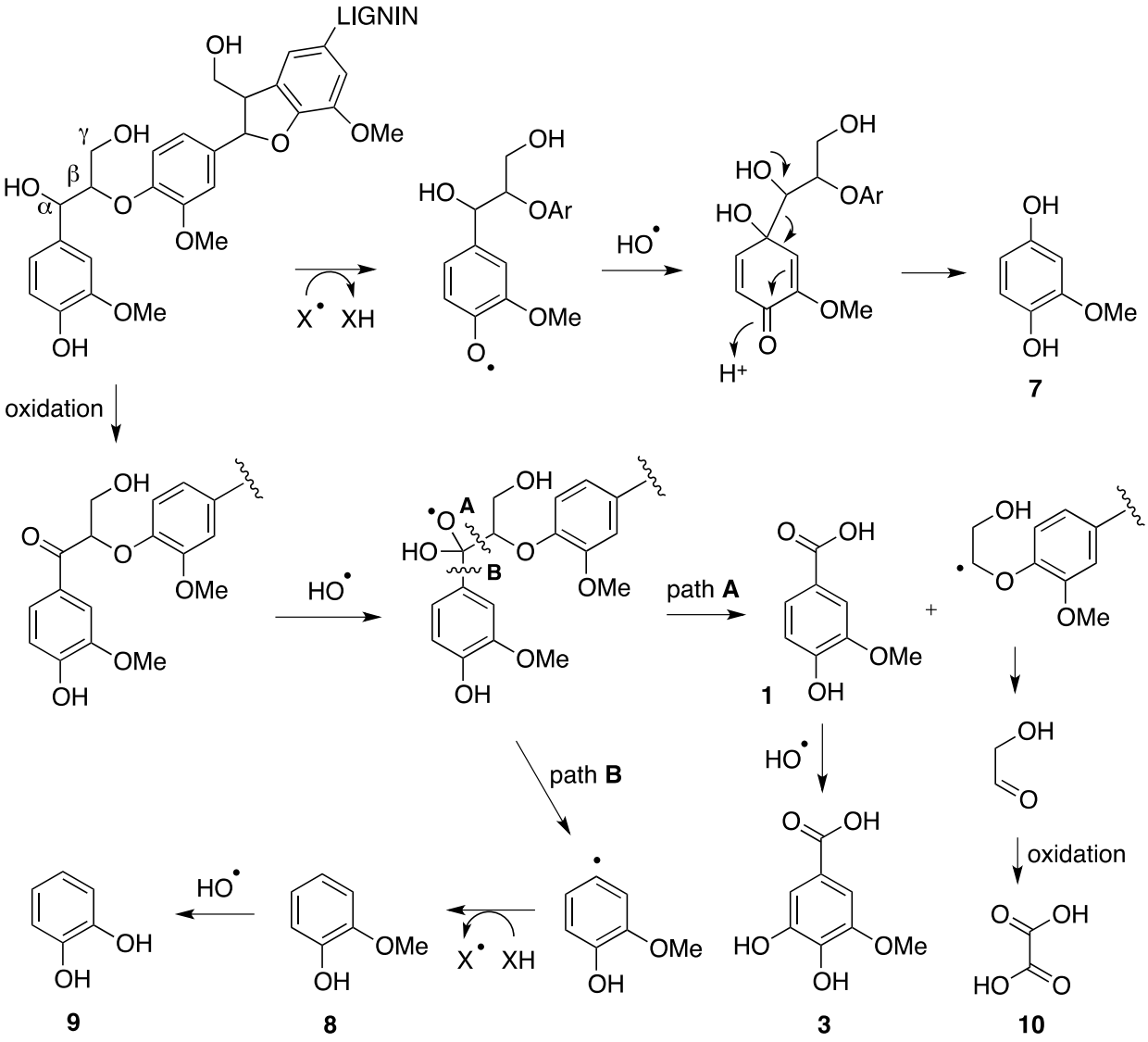
LIGNIN
OH
γ
β
α
HO
O
OMe
OMe
OH
X• XH
OAr
HO•
H+
7
oxidation
A
B
path A
path B
1
3
10
9
8